

Strong ground motions of the 2003 Bam Earthquake, Southeast of Iran (Mw=6.5)

Arash Jafargandomi^{1)*}, Sayed Mahmoud Fatemi Aghda²⁾, Sadaomi Suzuki¹⁾³⁾ and Takeshi Nakamura¹⁾

¹⁾ Department of Earth and Planetary Science, Faculty of Science, Kyushu University, Fukuoka, Japan

²⁾ Natural Disaster Research Institute of Iran, Tehran, Iran

³⁾ now, Tono Research Institute of Earthquake Science, Mizunami, Japan

Abstract

The acceleration waveforms of the mainshock of the 2003 Bam Earthquake, in southeast Iran (Mw=6.5) have been analyzed to derive several characteristics of strong ground motion. The near field effect of the main shock caused a huge maximum acceleration of about 1 G at the Bam station. Waveform analysis of this record shows a big effect of directivity with a strong motion in the fault normal direction. The fault normal component of the near field record shows a maximum displacement of about 30 cm. This effect is also shown when comparing the response spectrum of fault normal and fault parallel components of strong motion. The fault normal response spectrum shows a spectral displacement almost 2 times that of the parallel component, especially for periods greater than 1 s. The attenuation relations derived for both vertical and horizontal components have a very good correlation. Comparisons of the attenuation relation of the Bam earthquake with predictive attenuation relations in other regions (North of Iran, Turkey, and Japan) show a higher PGA gradient of decay in the Bam earthquake surrounding area. Calculations of duration of strong ground motion records show that up to 100 km strong motion duration increases with distance, and, after that, duration decreases. This could be explained by adding upper crust reflected waves up to 100 km, a weakening of wave amplitude, and decreasing total arrived energy at each station with distance increasing beyond 100 km. From a calculation of maximum displacements at all triggered stations the propagation pattern is also derived.

Key words: strong ground motion, Bam earthquake, attenuation relation, strong motion duration, directivity effect

1. Introduction

Since 1900, several big destructive earthquakes have occurred on the Iran plateau, which is one of the most earthquake-prone regions in the world. These earthquakes killed many people (Table 1) and several cities and villages were destroyed. In particular, 2 recent earthquakes, the 1990 Manjil and the 2003 Bam, have been remarkable.

The Bam earthquake (2003/12/26, Mw = 6.5), which occurred in southeast Iran is one of the most destructive earthquakes with about 30000 deaths.

The epicenter of this earthquake was reported by United States Geological Survey, USGS (29.004 N, 58.337 E) and Institute of Geophysics University of Tehran, IGUT (29.21 N, 58.40 E). Using aftershock distribution data, Suzuki *et al.* (2005) showed that the epicenter of the earthquake may be at Lat=29.050 E and Long=58.365 N with a hypocentral depth of 7 km. The most heavily damaged region of this earthquake was eastern Bam city. Baravat village, about 5 km east of the epicenter, suffered moderate damage. During this earthquake, the historic castle of Arg-e-

* e-mail: gandomi@geo.kyushu-u.ac.jp

Bam, the largest adobe (Mud Brick) complex in the world, was heavily damaged.

2. Recorded strong motions

Bam city is in Kerman Province in southeast Iran. There are 41 strong motion stations of the Building and Housing Research Center of Iran (BHRC) in Kerman Province. 32 stations use SSA2-type seismometers and 9 stations SMA-1-type seismometers. Among these stations, 24 were triggered and recorded seismic waves of the main shock. Table 2 shows a list of triggered stations and some strong motion parameters.

The maximum recorded ground acceleration is about 980 cm/s² in vertical component at Bam station in the middle of Bam city with an epicentral distance of about 7 km (Fig. 2). The minimum acceleration is

3.55 (cm/s²) of Bolvard station with an epicentral distance of 226 km (Table 2). A bandpass filter between 0.05 and 30–35 Hz is used to correct raw data. This filter has been chosen to increase the quality of accelerograms and reduce high-frequency noise by trial and error, and attention has been paid to having the least effect on the PGA value.

3. Analysis of seismic wave data

Among observed seismic wave data of the Bam earthquake, the record of Bam station in the Governmental Building is most important, because the highest acceleration might show a strong effect of the near field. The seismic waves of the main shock recorded at Bam station are shown in Fig. 3. As the original waveforms of acceleration are recorded as L, T, and V (Longitudinal, Transverse, and Vertical) components, we calculated the West-East and North-South components by rotating the co-ordinate of the horizontal L and T components. Among the 3 components of acceleration we can see that the vertical component contains a higher value of PGA, which is about 980 cm/s² and maximum velocity of about 110 cm/s on the West-East component and maximum displacement of about 30 cm also on the West-East component. This is because maximum acceleration and velocity are dominant at different frequencies when they appear on different components. Fig. 3 shows that the higher frequencies of about 8–10 Hz in

Table 1. Earthquakes with more than 1000 deaths in Iran since 1900 (data from USGS and IIEES)

Year	Month	Day	Latitude	Longitude	Depth(km)	M	Dead
1909	1	23	33.4	49.1	-	7.3	5500
1923	5	25	35.3	59.2	-	5.5	2219
1929	5	1	37.8	57.8	22	7.2	3257
1932	5	20	36.6	53.4	12	5.4	1070
1948	10	5	37.7	58.7	18	7.3	19800
1957	7	2	36.1	52.7	17	7.1	1200
1957	12	13	34.5	48	-	7.2	2000
1962	9	1	35.6	49.9	25	7.2	12225
1968	8	31	33.97	59.02	13	7.3	15000
1972	4	10	28.4	52.8	-	6.8	5010
1978	9	16	33.39	57.43	33	7.4	18220
1981	6	11	29.91	57.71	33	6.7	3000
1981	7	28	30.01	57.79	33	7.1	1500
1990	6	20	36.96	49.41	19	7.7	35000
1997	2	28	38.08	48.05	10	6.1	1100
1997	5	10	33.83	59.81	10	7.3	1572
2003	12	26	28.995	58.311	10	6.6	30000

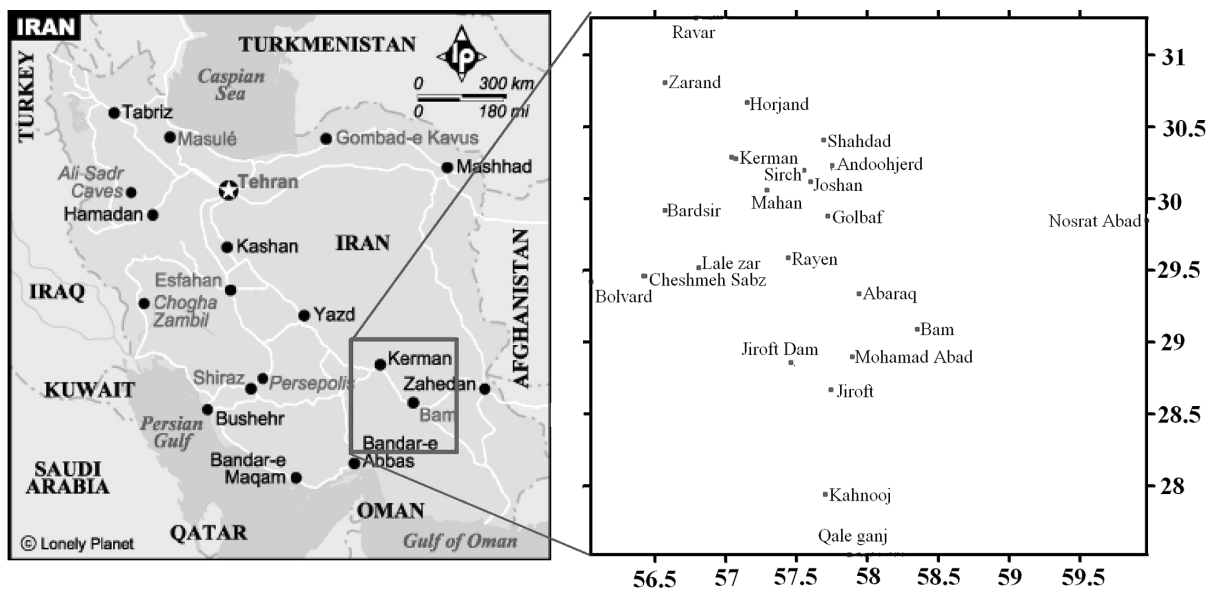


Fig. 1. Map of accelerograph stations in Kerman Province during the Bam earthquake.

Table 2. Characteristics of Strong Motion Records (BHRC, 2004)

NO.	STATION	Geographical Coordinates		PGA(cm/s/s)			Epicentral Dist (km)	Altitude m	Azimuth		Accelerograph Type
		E	N	L	V	T			L	T	
1	Bam	58.35	29.09	778.28	979.95	623.44	*	1094	278	8	SMA-1
2	Abaraq	57.94	29.34	166.69	83.81	109.47	49	1644	72	162	SSA2
3	Mohamad Abad	57.89	28.9	115.94	69.17	66.79	49	1961	350	80	SSA2
4	Jiroft	57.74	28.67	40.17	30.32	27.56	76	725	240	330	SSA2
5	Andoohjerd	57.75	30.23	31.82	14.07	33.59	139	851	200	290	—
6	Sirch	57.55	30.2	30.28	13.91	29.56	146	1685	30	120	SMA-1
7	Golbaf	57.72	29.88	30.29	12.8	27.65	107	1698	150	240	SSA2
8	Joshan	57.6	30.12	24.88	17.1	36.03	136	1650	142	232	SSA2
9	Kerman2	57.07	30.28	18.87	8.38	30.31	181	1755	140	230	SSA2
10	Kerman1	57.04	30.29	18.45	9.04	24.99	184	1767	175	265	SSA2
11	Qale Ganj	57.87	27.52	20.28	13.39	22.97	181	439	210	300	SSA2
12	Nosrat Abad	59.97	29.85	19.13	12.65	23.52	178	1115	284	14	SSA2
13	Kahnooj	57.7	27.94	10.75	7.76	10.54	143	556	20	110	SMA-1
14	Cheshme Sabz	56.42	29.46	22.85	9.11	10.71	192	2581	65	155	—
15	Rayen	57.44	29.59	14.61	14.67	13.91	104	2195	334	64	SMA-1
16	Shahdad	57.69	30.41	19.77	8.54	13.37	160	515	78	168	SMA-1
17	Bardsir	56.57	29.92	13.58	5.24	10.12	195	2113	75	165	SSA2
18	Mahan	57.29	30.06	11.99	7.8	13.46	149	1864	150	240	SSA2
19	Lale Zar	56.81	29.52	12.99	7.6	11.76	157	2822	65	155	SSA2
20	Ravar	56.79	31.26	11.99	6.08	12.11	284	1244	320	50	SMA-1
21	Zarand	56.57	30.81	12.1	6.21	12.52	257	1678	34	124	SSA2
22	Horjand	57.15	30.67	6.52	6.14	11.87	210	2320	110	200	SSA2
23	Bolvard	56.05	29.42	9.68	3.55	10.09	226	2088	145	235	SSA2
24	Jiroft Dam	57.46	28.86	20.92	10.33	11.99	90	1196	170	260	SSA2

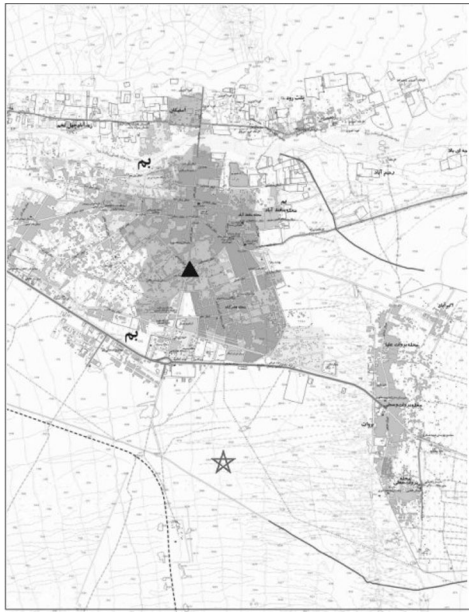


Fig. 2. Position of Bam accelerogram station (Black rectangle) and the epicenter of the mainshock (star, by Suzuki *et al.*, 2004).

the vertical component are dominant, which may be due to the presence of P waves. The lower frequencies of about 5Hz are dominant in the horizontal

component. On the West-East component a peak of the Fourier spectrum at lower frequencies may be due to the near field directivity effect. It made high-amplitude and low-frequency waves especially in fault normal direction.

We show a 2-D view of particle motions for 2.5, 5, and 7.5 seconds of particle motion at Bam station (Fig. 4). The W-E component of displacement, which shows the maximum amplitude of 30 cm, is more prominent than the N-S and vertical components.

In Fig. 4 we can see that the first particle motion was toward the west and then toward the east, which all show about a 50 cm displacement in the west-east direction (almost fault normal) and a total displacement of about 30 cm in north-south direction (Fig. 4 c). Fig. 4d shows a vertical slice in west-east direction with about 13 cm vertical displacements.

To roughly estimate the site effect on the maximum value of strong motion, the V_{max}/a_{max} ratio may be used. As the maximum values of velocity and acceleration usually depend on different frequencies, this ratio may depend on the frequency content of ground motion. V_{max}/a_{max} is the dominant period of waves at a specific station (McGuier 1978). For Bam

Table 3. Site classification depending on V_{max}/a_{max} ratio (Seed and Idriss1982)

V_{max}/A_{max}	Site Condition
0.056 Sec	Rock
0.112 Sec	Hard Soils (<200 ft)
0.138 Sec	Deep Hard Soils (>200 ft)

station this ratio is equal to 0.133 to 0.143s for the horizontal components, hence the dominant period at this station would be about 0.84s. Idriss and Seed (1982) proposed values for different site conditions at epicentral distances up to 50 km (Table 2). According to this classification a V_{max}/a_{max} ratio equal to 0.133–0.143s for Bam station classifies this site in the third group (Deep Hard Soils >200 ft).

4. Strong motion attenuation

The attenuation pattern of strong motion has been derived from recorded accelerograms. Fig. 6 shows the relationship between acceleration and epicentral distance for vertical and horizontal components. The value for horizontal acceleration is the arithmetic mean of 2 horizontal components. For curve fitting to acceleration data we used the equation:

$$\ln A = a + b \ln X$$

A shows the acceleration amplitude and X is the epicentral distance. a and b are coefficients of the regression equation (ln is natural Log). We derived this equation for both vertical and horizontal components (Table 4). In this table the higher value of the b coefficient for the vertical component shows faster attenuation of the vertical component of acceleration than the horizontal component. The higher value of the standard error for the horizontal component shows that the horizontal component is more sensitive to local site effects. Fig. 5 shows that for all stations except Bam station horizontal acceleration is larger than vertical acceleration.

4.1. Comparison with other studies

In Fig. 6 the attenuation of horizontal PGA for the Bam earthquake is compared to the predictions of Ozel *et al.* (2004) for the aftershock ($M_w=5.8$) of the 1990 Izmit earthquake in Turkey and Fukushima and Tanaka (1990) using a data base of 1372 horizontal

components from 28 earthquakes in Japan and 15 earthquakes in the United States. Because the magnitude of the Bam earthquake is 6.5, this magnitude has been assigned to these attenuation relations for comparison. It is evident that the predicted near-source horizontal PGA for the Bam earthquake using the equation derived in this study is higher than the others at distances of less than about 30 km. We can see the same situation for distances of more than about 100 km. But, for distances of between 30 and 100 km the predicted attenuation using the Fukushima and Tanaka equation for Japan shows higher values. Also, Niazi and Bozorgnia (1992) derived the attenuation relation of PGA for the 1990 Manjil, north of Iran, earthquake ($M_s=7.7$). They derived the b of the attenuation relation of horizontal PGA, which shows the gradient of PGA decay between -1.02 and -1.07 and for vertical PGA between -1.07 and -1.13 . In this study we derived the b value equal to -1.099 for horizontal and -1.407 for vertical PGA. These show higher values for the PGA decay gradient both in horizontal and vertical components compared to the Manjil earthquake.

5. Strong motion duration

There are several definitions of strong motion duration. Here, we use the definition proposed by Husid *et al.* (1969). This is the time interval in which 90% of the total energy arrives at the recording station. We calculated the energy received at between 5% and 95%.

$$Energy = \int_t f(t)^2 dt$$

$$Duration = t_{95\%} - t_{5\%}$$

Where $f(t)$ is the acceleration and $t_{95\%}$ and $t_{5\%}$ are time for receiving 95% and 5% of total energy. The duration is calculated for all records of both vertical and horizontal components. The results are shown in Fig. 7 for vertical and arithmetic mean of 2 hori-

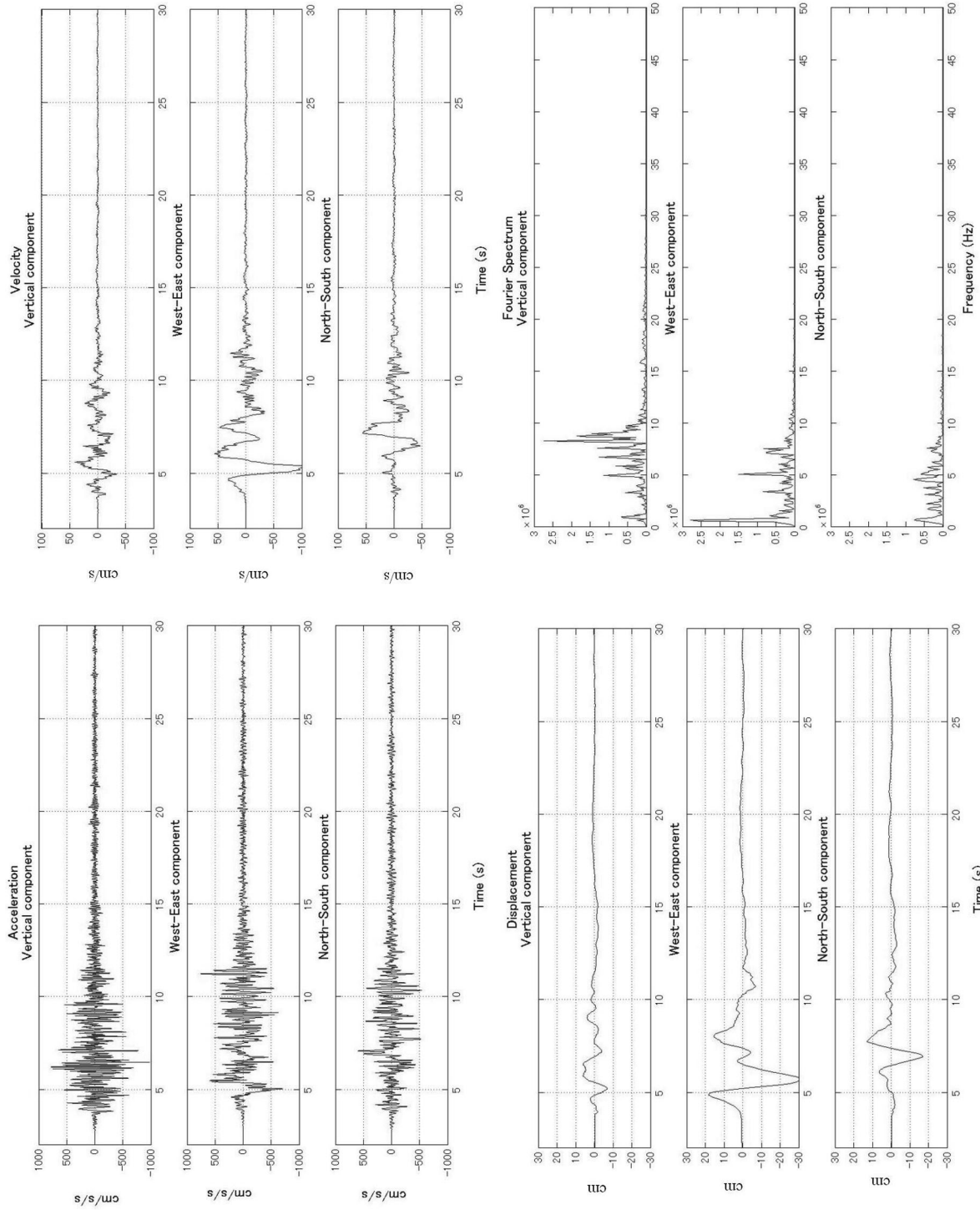


Fig. 3. Acceleration and calculated velocity and displacement components of the seismic wave of the mainshock observed in Bam station. Fourier spectrum of acceleration is also shown at lower right (original Acceleration data are presented by BHRC 2004).

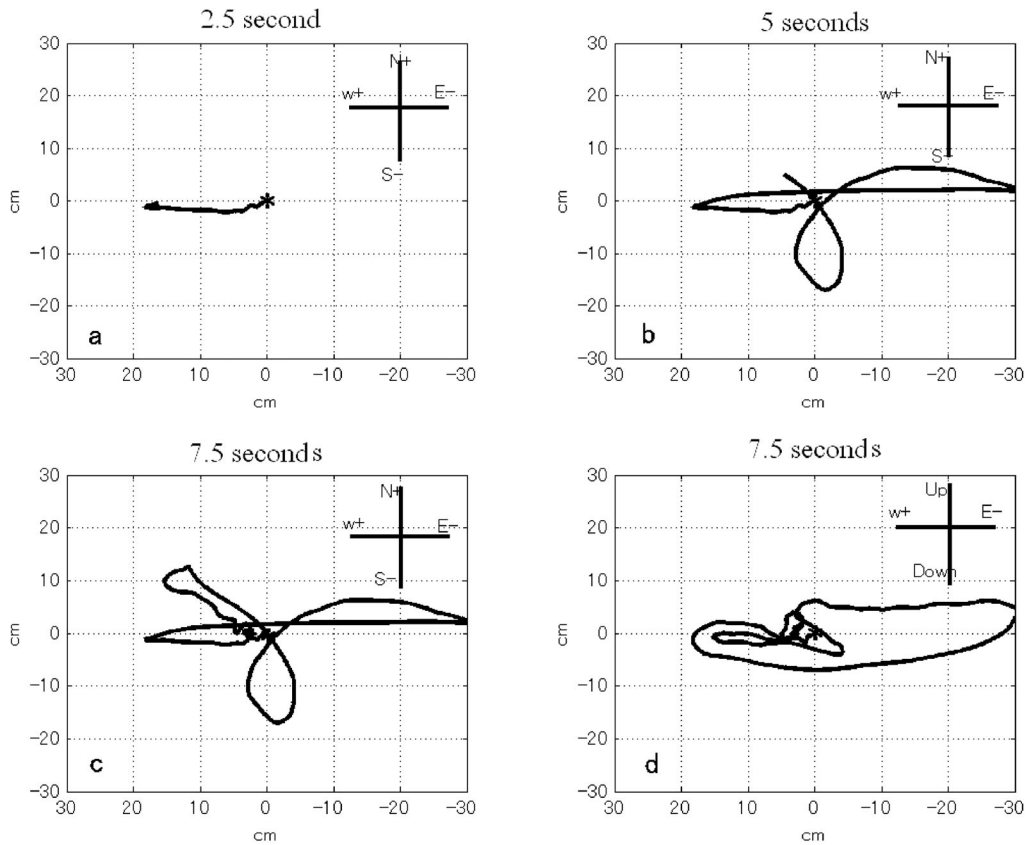


Fig. 4. 2-D particle motion of displacement for the mainshock observed at Bam station.

Table 4. Acceleration attenuation parameters

Parameter	component	
	Vertical	Horizontal
<i>a</i>	9.6269	8.694
<i>b</i>	-1.4075	-1.099
<i>Std. Er</i>	6.828	15.6314
<i>R</i>	0.999	0.994

a and *b* are regression coefficients
Std. Er is standard error
R is correlation coefficient

zontal components. As shown in Fig. 7, the strong motion duration increases as the epicentral distance increases up to about 100 km. But, after about 100 km the duration decreases. Novikova and Trifunak (1993) suggested that a strong motion duration depends on frequency, and different frequencies show different durations. They used 494 strong motion records in California since 1933. They studied the dependency of strong motion duration on different parameters such as magnitude, local geology, and also epicentral distance. They showed that as epicentral distance increases the duration increases, but for

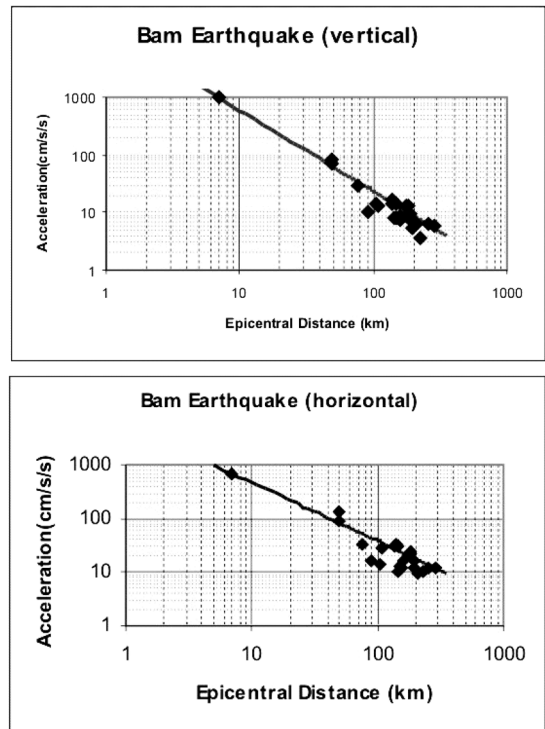


Fig. 5. Attenuation regression curve; up: vertical component. Down: horizontal components.

longer distances as the signals are weakening, and this causes the late triggering of recorders, so the duration of recorded strong motion decreases. The increase of duration up to 100 km may be the result of

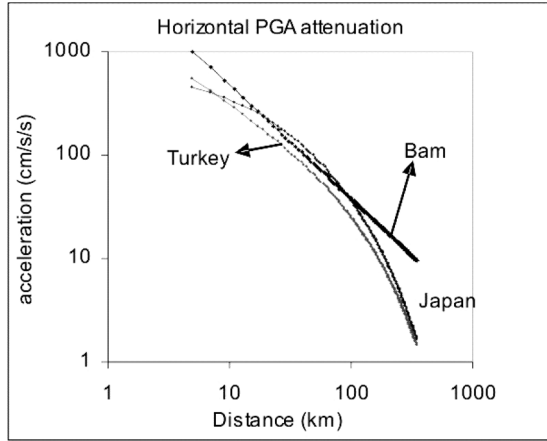


Fig. 6. Comparison of Bam attenuation of horizontal PGA with M6.5 predictive curves of Ozel *et al.* (2004) for Turkey and Fukushima and Tanaka (1990) for Japan.

increases in complex upper crust reflection waves. The decrease after 100 km could be the result of seismic wave attenuation. Up to about 100 km, the durations of both vertical and horizontal components are almost the same. But, after 100 km, the vertical component shows higher values for duration.

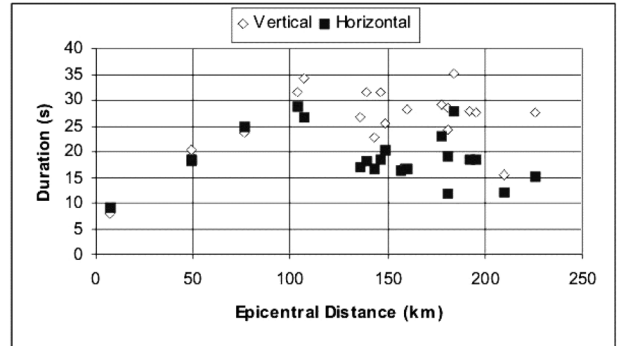


Fig. 7. Strong motion duration of vertical and horizontal components.

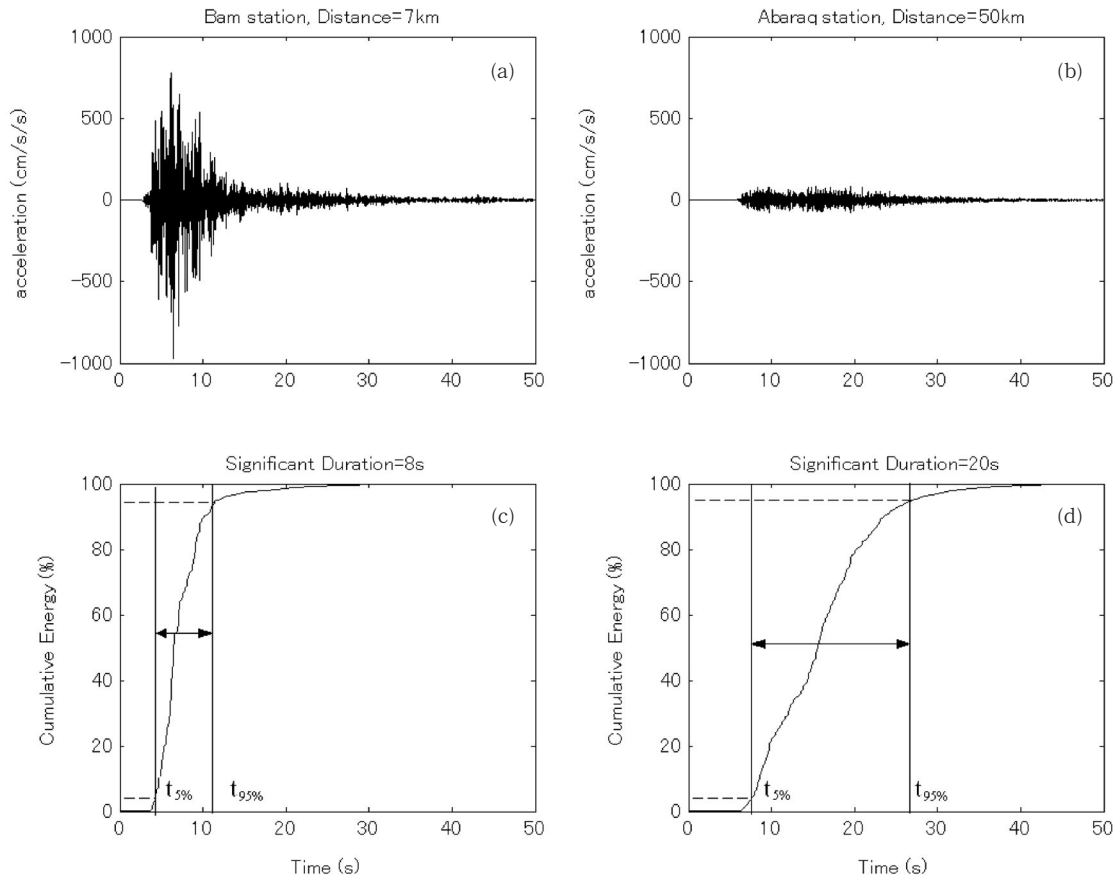


Fig. 8. Strong motion duration for vertical component of Bam station record (a) and Abaraq station record (b). These energy functions for calculating duration are also shown in (c) and (d).

Figure 8 shows vertical components of 2 records from Bam station and Abaraq station. The epicentral distances of Bam and Abaraq stations are 7 km and 50 km, respectively. For these 2 records, the cumulative summation of acceleration squares which we call energy of accelerogram is calculated. We can see that the slope of the energy function for Abaraq station with a larger epicentral distance is lower than that for Bam station. According to definition of the strong motion duration, Abaraq station has a longer duration of strong motions than Bam station. The strong motion durations of the vertical component for Bam station and Abaraq station are about 8 s and 20 s, respectively.

6. Rupture directivity effect

Generally, the earthquake source is a shear dislocation that begins at a point on a fault and spreads. The propagation of fault rupture toward a site with a velocity close to the shear wave velocity causes a single large pulse of motion, which is recorded at the beginning (Somerville *et al.*, 1997). This pulse of motion represents the cumulative effect of almost all of the seismic radiation from the fault. The directivity effect is affected by epicentral distance, angle between source, and site and magnitude (Somerville *et al.*, 1997, Somerville 2003, Miyake *et al.* 2001). The forward rupture directivity effect occurs when both directions of seismic wave propagation toward the site and rupture propagation of slip on the fault are aligned with the site. This directivity effect can be seen in the case of the Bam earthquake. Suzuki *et al.* (2005) and Nakamura *et al.* (2004) introduced the blind fault, which ruptured during the Bam earthquake using aftershock distribution. This blind fault passes through the eastern part of Bam city in almost the north-south direction (Fig. 9).

Generally, forward directivity generates different waveforms between fault normal and fault parallel directions. As shown in Figs. 3 and 4 the seismic waveform of the Bam earthquake observed by Bam station represents such a difference. The displacement normal to the fault (west-east component) is nearly 2 times that parallel to the fault (north-south component). Also, a 2-D view of the particle motion of horizontal displacement shows this phenomenon (Fig. 4). Somerville *et al.* (1997) showed the forward rupture directivity effect in the 1992 Landers earth-

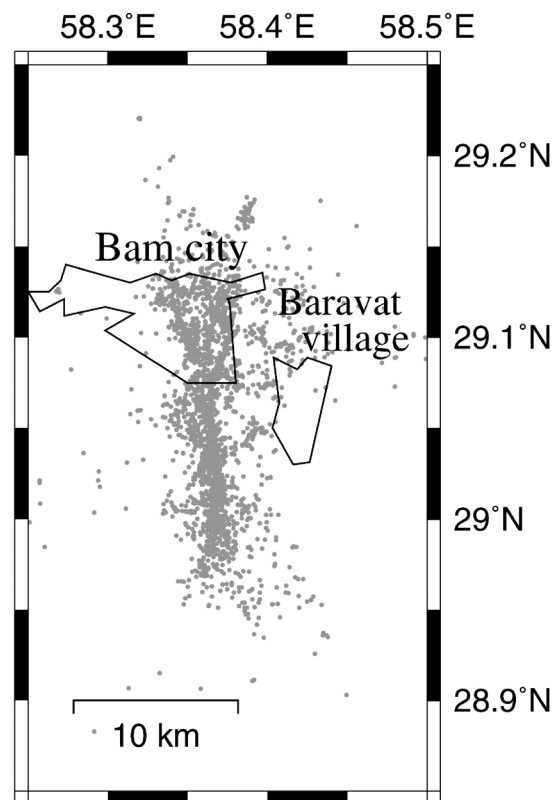


Fig. 9. Source fault of Bam earthquake derived from aftershock distribution (Suzuki *et al.*, 2005).

quake for 2 stations at Joshua Tree near the epicenter and Lucerens in the direction of rupture propagation, but farther.

We can see the rupture directivity effect on the map of the damaged area presented by National Cartographic Center (NCC) of Iran. Fig. 10 presents a comparison of the heavily damaged area in Bam city and the relatively lightly damaged area in Baravat village. This map shows that the distances of 2 areas from the epicenter are nearly the same, but the damage in Bam city is heavier than that of Baravat village.

Considering the 2-dimensional view of particle displacement at Bam station (Fig. 4), we can see a larger displacement in the fault normal compared to the fault parallel. This figure shows about a 50 cm fault normal and about a 30 cm fault parallel component displacement. Abrahamson and Silva (1997) and Somerville (1997) suggested that the directivity effect on main strong motion can be affected in the response spectrum. This is shown in Fig. 11, which shows a comparison of the response spectrum for

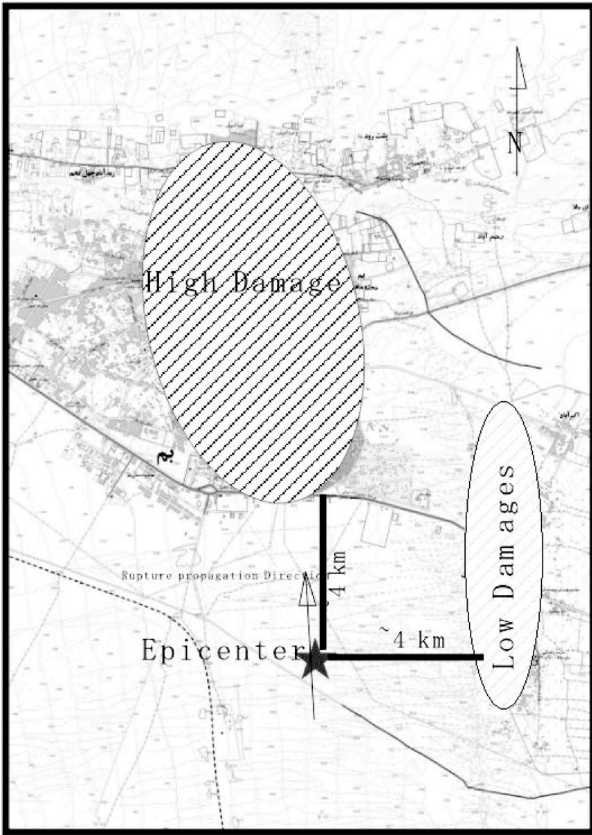


Fig. 10. Position of low and high damage area with respect to epicenter.

fault normal and fault parallel components. This figure shows a higher value for the fault normal component for periods of more than 0.8 second, and especially from 1.2 seconds, which is about 2 times bigger. Also, Somerville (1997) showed the directivity effect in the 1992 Landers earthquake for near field records. He showed a higher value for the fault normal response spectrum for which the difference also increased with increasing periods.

7. Effect of rupture directivity on propagation pattern

Figure 12 shows a graph of the maximum displacements for the seismic stations versus their radiation azimuths from the epicenter. The displacements were calculated from their recorded accelerograms. These data show that the maximum displacement is recorded for an angle (The angle is measured between site and source from rupture direction which is northerly, anticlockwise) of about 45 degrees. In this figure 2 peaks can be seen, one around

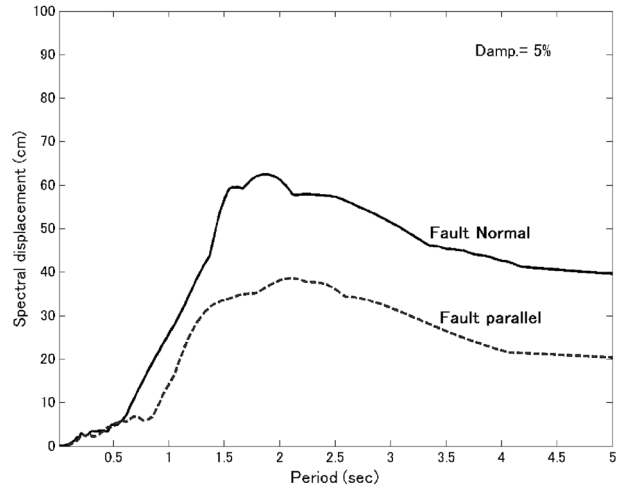


Fig. 11. Comparing fault normal and fault parallel response spectrum.

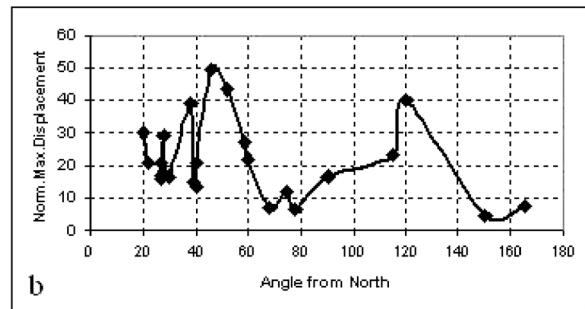
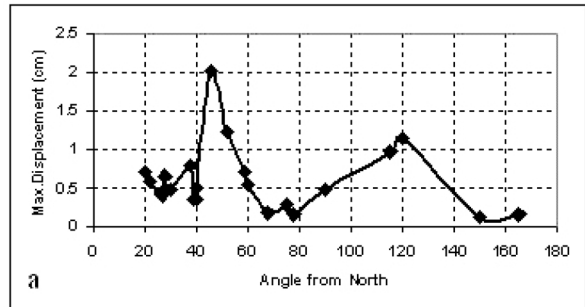


Fig. 12. Variation of maximum displacement with angle. a) Uncorrected data b) Corrected data with respect to distance.

45 degrees and the other around 120 degrees. The first peak with smaller angle might be related to the rupture direction. And the second peak may be related to the far field effect of the rupture directivity.

To remove the effect of distance we corrected the data with respect to epicentral distance. For this correction we used the geometrical spreading factor G . This factor shows the geometric decay of seismic wave amplitude with increasing distance and is de-

Table 5. Characteristics of selected station for far field directivity effect.

Station	Epic.Dist(km)	Angle	a(L)	a(v)	a(T)	Surface Geology
Abaraq	49	46	166.69	83.81	109.47	Evaporites and alluvial traces
Mohamad Abad	49	115	115.94	69.17	66.79	Young Alluvial fans
Golbaf	107	30	30.29	12.8	27.65	Soils with modarate strenght
Rayen	104	52	14.61	14.67	13.91	Conglumarate and sandstone
Sirch	146	27	30.28	13.91	29.56	Quaternary Alluvium
Kahnooj	143	150	10.75	7.76	10.54	Silt and fine grain alluvium

finied as:

$$G = \frac{R_0}{R^n}$$

R is epicentral distance and R_0 is unit distance (1 km), and n depends on distance. Lam *et al.* (2000) showed the variation of the geometrical spreading factor G with distance as follows:

$$G = \frac{R_0}{R} \quad \text{for } R \leq 70 \text{ km}$$

$$G = \frac{R_0}{70} \quad \text{for } 70 \leq R \leq 130 \text{ km}$$

$$G = \frac{R_0}{70} \sqrt{\frac{130}{R}} \quad \text{for } R \geq 130 \text{ km}$$

To correct observed data, the maximum value calculated from observed acceleration is divided by G (Fig. 12 b).

Through a comparison of the same epicentral distance stations in different directions we show the propagation directivity effect on far fields where the strong ground motions of the Bam earthquake were recorded. We selected 3 pairs of stations with nearly equal epicentral distances for each pair (Table 5). (The angle is measured between site and source from rupture direction which is northerly anticlockwise). Fig. 13 shows the comparison between recorded accelerations for 3 components. A comparison of these stations also shows that even the surface geology of each station affects the maximum recorded acceleration on the angle with respect to rupture propagation direction.

8. Conclusions

Using strong motion data recorded by BHRC we analyzed the strong motion characteristics of the Bam earthquake. The near field waveform analysis shows a clear directivity effect. This effect causes higher values of acceleration, velocity, and displace-

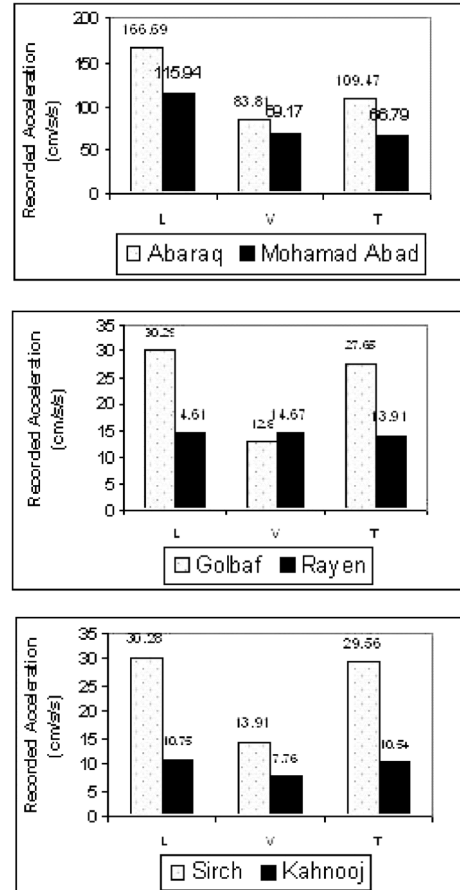


Fig. 13. Comparison of observed acceleration in equal distance stations with different azimuthal position for three components (L, V and T).

ment in the fault normal direction. After obtaining the driving attenuation relation of PGA from recorded strong motions, it is compared with other attenuation relations of other regions. The result shows a higher value of PGA decay gradient in the epicentral area of the Bam earthquake and its surrounding. This comparison has been done for northern Iran and also predictive attenuation relations of Turkey and Japan, which are both high earthquake hazard risk regions.

The calculation of strong motion duration shows that as distance increases up to 100 km the duration increases more than could be due to additions of crustal reflections and surface waves with increasing epicentral distance. For distances beyond 100 km the strong motion duration decrease can be due to signal weakening for very large epicentral distances. The driving wave propagation pattern obtained using far field recorded data shows that the rupture directivity also can be deduced from far field data.

Acknowledgment

We greatly appreciate the assistance of Building and Housing Research Center (BHRC) of Iran for preparing the raw accelerograms data. We are also grateful for help and support from the members of Natural Disaster Research Institute of Iran and Seismological laboratory, Department of Earth and Planetary Sciences, Kyushu University. We also thank professor Furumura for his valuable comments to improve the article.

References

- Abrahamson, N.N. and W.J. Silva, 1997, Empirical response spectral attenuation relations for shallow crustal earthquakes, *Seismological Research Letters*, **68**, 1, 94-127.
- BHRC Report No. 280, 1998, Characteristics of national strong motion network, 107 p.
- Fukushima, Y. and T. Tanaka, 1990, A new attenuation relation for peak horizontal acceleration of strong earthquake ground motion in Japan, *Bull. Seism. Soc. Amer.*, **80**, 757-783.
- Kramer, S.L., 1995, Geotechnical earthquake engineering, *Pearson Education*, 653 p.
- Lam, N., J. Wilson and G. Hutchison, 2000, Generation of synthetic earthquake accelerograms using seismological modeling: *A Review. Journal of earthquake engineering*, **4** (3): 321-354.
- McGuire, R.K., 1978, Seismic ground motion parameter relations, *Journal of Geotechnical Engineering Division*, ASCE, **104**, No. GT4, 481-490.
- Miyake, H., T. Iwata and K. Irikura, 2001, Estimation of rupture propagation direction and strong motion generation area from azimuth and distance dependence of source amplitude spectra, *Geophysical Research Letters*, **28** (14), 2727-2730.
- Nakamura, T., S. Suzuki, H. Sadeghi, S.M. Fatemi Aghda, T. Matsushima, Y. Ito, S.K. Hosseini, A. Jafargandomi and M. Maleki, 2005, Source fault of the 2003 Bam, South-eastern Iran, earthquake Mw 6.5 inferred from the after-shock distribution and it's relation to heavily damaged area: existence of Arg-e-Bam fault proposed, (Submitted to GRL).
- Niazi, M. and Y. Bozrgnia, 1992, The 1990 Manjil, Iran, earthquake: Geology and seismology overview, PGA attenuation, and observed damage, *Bull. Seism. Soc. Amer.*, **82**, 774-799.
- Novikowa, E.I. and M.D. Trifunac, 1993, Duration of strong earthquake ground motion: physical basick and empirical equations, *Report No.CE 93-02, University of Southern California*, 259 p.
- Ozel, N.M., T. Sasatani and O. Ozel, 2004, Strong ground motion during the largest aftershock (Mw=5.8) of the 1999 Izmit earthquake, Turkey, *Tectonophysics*, **391**, 347-355.
- Seed, H.B. and I.M. Idriss, 1982, Ground motion and soil liquefaction during *Earthquakes, Earthquake Engineering Research Institute*, Berkeley, California, 134 p.
- Somerville, P.G. 2003, Magnitude scaling of the near fault rupture directivity pulse, *Physics of the Earth and Planetary Interior*, **137**, 201-212.
- Somerville, P.G., N.F. Smith, R.W. Graves and N.A. Abrahamson, 1997, Modification of empirical strong ground motion attenuation relations to include the amplitude and duration effects of rupture directivity, *Seismological Research Letters*, **68**, 1, 199-222.
- Suzuki, S., T. Matsushima, Y. Ito, S.K. Hosseini, T. Nakamura, A. JafarGandomi, H. Sadeghi, M. Maleki, and S.M. Fatemi Aghda, 2004, Source fault of the 2003/12/26 Bam earthquake (Mw6.5) in southeastern Iran inferred from aftershock observation data by temporal high-sensitive-seismograph network, *AGU 2004 Joint Assembly, Montreal*.

(Received January 14, 2005)

(Accepted February 21, 2005)